

Research Article

Simplex Cubature Kalman-Consensus Filter for Distributed Space Target Tracking

Zhaoming Li ¹, Wenge Yang ², Dan Ding ² and Yurong Liao²

¹Graduate School, Space Engineering University, Beijing 101416, China

²Department of Electrical and Optical Engineering, Space Engineering University, Beijing 101416, China

Correspondence should be addressed to Dan Ding; ddnjr@163.com

Received 11 January 2018; Accepted 15 April 2018; Published 24 June 2018

Academic Editor: Pavlos I. Lazaridis

Copyright © 2018 Zhaoming Li et al. This is an open access article distributed under the Creative Commons Attribution License, which permits unrestricted use, distribution, and reproduction in any medium, provided the original work is properly cited.

A simplex cubature Kalman-consensus filter, which is suitable for distributed space target tracking using multiple radars, is proposed to improve the target tracking accuracy. The detailed orbital dynamics model and radar measurement model are given as the system filtering models. The intractable nonlinear Gaussian weighted integral in the filter is decomposed into the spherical integral and radial integral, which are calculated using the spherical simplex rule and the second-order Gauss-Laguerre quadrature rule, respectively. In this way, a new simplex cubature rule is derived. By means of the statistical linear regression method, the posterior mean, covariance, and the transmitted messages in the extended Kalman-consensus filter are approximated using the deduced simplex cubature rule, which results in the proposed simplex cubature Kalman-consensus filter. No data fusion center exists in the filter, and each radar only needs to exchange the information with its neighbors to reach a consensus estimate. The simulation results show that the proposed filter can achieve more accurate results compared with the cubature Kalman-consensus filter.

1. Introduction

In recent years, the orbital resources are becoming increasingly strained on account of the increase in the number of space targets, which should be monitored to improve the utilization efficiency of the space resources. Ground-based radar is a significant sensor in the space surveillance system, it provides round the clock working capability, and it is a key technology to use its measurement data for space target tracking [1].

The space target tracking can be considered as a nonlinear system state estimation problem, and two methods, including the particle filter and the nonlinear Kalman filter, are mainly taken. Particle filter is a type of Monte Carlo based filter, which is theoretically applicable to arbitrary nonlinear non-Gaussian system without any assumptions on the posterior probability density function (PDF) [2]. However, in practical applications, there appear some problems containing particle degradation and depletion, large amount of calculation, and the choice of the importance function that will affect the

filtering accuracy as well as the computational efficiency [3]. Therefore it is not suitable for application in the occasion that requires high real-time performance [4].

In the nonlinear Kalman filter, the posterior PDF is assumed to be Gaussian distribution, and the suboptimal estimate of the nonlinear system state is obtained. The extended Kalman filter (EKF) [5] is the most widely used nonlinear Kalman filter in the past several decades, it uses the multidimensional Taylor series expansion to linearize the nonlinear function, and then the standard Kalman filter is applied. For arbitrary nonlinear transformation, it can be seen using the Taylor series that the linearized mean can only match to the first order of the true one; hence the EKF is considered to achieve the first-order filtering accuracy. Moreover, the accuracy and the numerical stability of EKF are reduced for the strong nonlinear system, and the calculation of Jacobian matrix imposes further restrictions on the system models.

Based on the assumption that the approximation to the posterior PDF is easier than that of arbitrary nonlinear

function, Julier [6] proposed the unscented Kalman filter (UKF). UKF is a deterministic sampling filter; that is, the posterior mean and covariance are calculated using the sampling points, which are generated using the nonlinear propagation of sigma points selected as certain criterion, and the third-order accuracy can be achieved [7]. UKF is a derivation-free filter, which can commendably overcome the defects of EKF. However, there exist some tunable parameters in sigma points, the selection of which lacks rigorous mathematical basis, and the negative weight on the center point may reduce the numerical stability for high-dimensional system [8, 9].

By means of the coordinate transformation, Arasaratnam [10] proposed the cubature Kalman filter (CKF), in which the key intractable integral is decomposed into the spherical integral and radial integral. These two integrals are approximated using different numerical methods, respectively, and result in the spherical-radial cubature rule, which is used to calculate the posterior mean and covariance in the nonlinear Kalman filter framework. CKF can be regarded as a special case of UKF with the parameter $\kappa = 0$ [11], whereas CKF gives the rigorous mathematical reason why κ should be chosen zero for the first time. Furthermore, CKF has higher numerical stability than UKF and has a wide range of applications in engineering [12, 13].

In order to further improve the estimation accuracy of CKF, Wang [14] introduced the transformation group of the regular simplex to compute the spherical integral and proposed the spherical simplex-radial cubature Kalman filter (SSRCKF). The simulation results show that SSRCKF can achieve more accurate results compared with CKF for high-dimensional system. Bhaumik [15, 16] adopts n -order generalized Gauss-Laguerre quadrature rule to calculate the radial integral and puts forward the cubature quadrature Kalman filter (CQKF). It is pointed out that CQKF is the generalized form of CKF; that is, CKF is the simplified form of CQKF with the first-order Gauss-Laguerre quadrature rule. Jia [17] proposes the higher-order cubature Kalman filter; it improves the filtering accuracy with much more points needed.

However, the space target tracking accuracy obtained by a single radar cannot satisfy the demands in some practical applications; thus the information fusion by multiple radars should be considered. In tradition, the information is centralized fused; namely, all radars send their measurement data to a data fusion center, on which the centralized filter is carried out. In this mode, the whole system will collapse once the center failure occurs. With the development of distributed sensor network technology, distributed filter has become a subject undergoing intense study [18, 19]. Olfati [20, 21] gives a computational framework of the Kalman-consensus filter (KCF) for linear system, in which multiple sensors synchronously observe the same target, and the estimation errors among local nodes are eliminated through information collaborative interaction, such that the state estimates of various sensors reach a consensus. Furthermore, a consensus-based distributed Kalman filter for state estimation in a sensor network considering the random failures of the connections is proposed in [22], and a Kalman filter of type consensus+innovations distributed linear estimator of

the linear time-invariant dynamical systems is developed in [23]. These two distributed filters have shown better performance compared with KCF in some cases; however, they are designed for linear systems. For nonlinear system, Pellett [24] proposes the extended Kalman-consensus filter; nevertheless, the filter holds the inherent defects of EKF, that is, to calculate the Jacobian matrix and achieve the first-order accuracy.

In this paper, a simplex cubature Kalman-consensus filter (SCKCF) is put forward to improve the distributed space target tracking accuracy by multiple radars. First, for the intractable nonlinear Gaussian weighted integral, the spherical simplex rule and the second-order Gauss-Laguerre quadrature rule are utilized to calculate the spherical integral and radial integral, respectively, and a new simplex cubature rule is derived. Then, combined with the statistical linear regression method, the SCKCF is proposed in the extended Kalman-consensus filter framework. Different from the centralized filter, there is no data fusion center in the SCKCF, and each radar only exchanges information with its neighbors, which can effectively improve the system's fault tolerance and scalability. The simulation results show that the proposed SCKCF can achieve higher orbit determination accuracy than cubature Kalman-consensus filter.

The rest of this paper is organized as follows: the mathematical models for space target tracking are provided in Section 2. The new simplex cubature rule is derived in Section 3. The simplex cubature Kalman-consensus filter is proposed in Section 4. The simulation results and analysis are presented in Section 5. The conclusion is given in Section 6.

2. Mathematical Models for Space Target Tracking

In this section, the space target orbital dynamics model and the radar measurement model, which are considered as the state equation and measurement equation in the filter, respectively, are given below.

2.1. The Orbital Dynamics Model. The space target orbit is described in the J2000 earth inertial coordinate system ($O - XYZ$, shown in blue in Figure 1), and the orbital dynamics model with J_2 nonspherical gravitational perturbation is given as follows:

$$\begin{aligned}
 \dot{x} &= v_x \\
 \dot{y} &= v_y \\
 \dot{z} &= v_z \\
 \dot{v}_x &= \frac{\mu x}{r^3} \left[J_2 \left(\frac{R_e}{r} \right)^2 \left(7.5 \frac{z^2}{r^2} - 1.5 \right) - 1 \right] + f_x \\
 \dot{v}_y &= \frac{\mu y}{r^3} \left[J_2 \left(\frac{R_e}{r} \right)^2 \left(7.5 \frac{z^2}{r^2} - 1.5 \right) - 1 \right] + f_y \\
 \dot{v}_z &= \frac{\mu z}{r^3} \left[J_2 \left(\frac{R_e}{r} \right)^2 \left(7.5 \frac{z^2}{r^2} - 4.5 \right) - 1 \right] + f_z \\
 r &= \sqrt{x^2 + y^2 + z^2}
 \end{aligned} \tag{1}$$

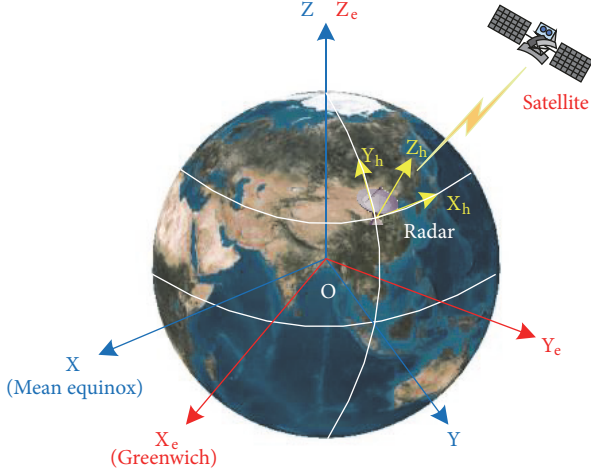


FIGURE 1: The coordinate systems.

where $\mathbf{X}_p = (x, y, z)^T$ and $\mathbf{X}_v = (v_x, v_y, v_z)^T$ denote the position and velocity of the space target, respectively. The parameters J_2 , μ , and R_e represent the harmonic coefficient, the earth gravitational constant, and the radius of the earth, respectively. The perturbation $(f_x, f_y, f_z)^T$ is the sum of the high-order nonspherical perturbation, three-body gravitational perturbation, and solar radiation pressure perturbation, which can be considered as the zero mean white Gaussian noise in this study.

Equation (1) can be written in the following discrete form by using the fourth-order Runge- Kutta method:

$$\mathbf{X}_k = \mathbf{f}(\mathbf{X}_{k-1}) + \mathbf{w}_{k-1} \quad (2)$$

where $\mathbf{X}_k = (\mathbf{X}_{p,k}^T, \mathbf{X}_{v,k}^T)^T = (x_k, y_k, z_k, v_{x,k}, v_{y,k}, v_{z,k})^T$ denotes the orbit state at time k , \mathbf{w}_{k-1} represents the process noise at time $k - 1$, and $\mathbf{f}(\cdot)$ is the nonlinear function in (1).

2.2. The Measurement Model. The measurement model is established in the radar horizon coordinate system ($O - X_h Y_h Z_h$, the yellow one in Figure 1), in which the orbital state is expressed as $\widehat{\mathbf{X}}_k = (\widehat{\mathbf{X}}_{p,k}^T, \widehat{\mathbf{X}}_{v,k}^T)^T$, where $\widehat{\mathbf{X}}_{p,k} = (\widehat{x}_k, \widehat{y}_k, \widehat{z}_k)^T$ and $\widehat{\mathbf{X}}_{v,k} = (\widehat{v}_{x,k}, \widehat{v}_{y,k}, \widehat{v}_{z,k})^T$. And the geometrical relationships between the range R_k , velocity \dot{R}_k , azimuth angle A_k , elevation angle E_k of radar, and orbital state are given as follows:

$$R_k = \sqrt{\widehat{x}_k^2 + \widehat{y}_k^2 + \widehat{z}_k^2}$$

$$\dot{R}_k = \frac{(\widehat{x}_k \widehat{v}_{x,k} + \widehat{y}_k \widehat{v}_{y,k} + \widehat{z}_k \widehat{v}_{z,k})}{\sqrt{\widehat{x}_k^2 + \widehat{y}_k^2 + \widehat{z}_k^2}}$$

$$A_k = \arctan \frac{\widehat{y}_k}{\widehat{x}_k}$$

$$E_k = \arctan \frac{\widehat{z}_k}{\sqrt{\widehat{x}_k^2 + \widehat{y}_k^2}}$$

(3)

However, the orbital model and the measurement model are established in $O - XYZ$ and $O - X_h Y_h Z_h$, respectively, and it is required to perform a coordinate transformation, the detailed process of which is listed in Appendix. Consequently, (3) can be written in the following measurement equation form.

$$\mathbf{Z}_k = \mathbf{h}(\mathbf{X}_k) + \mathbf{v}_k \quad (4)$$

where $\mathbf{Z}_k = (R_k, \dot{R}_k, A_k, E_k)^T$ denotes the measurement element at time k , \mathbf{v}_k represents the measurement noise at time k , and $\mathbf{h}(\cdot)$ is the nonlinear function in (3).

3. Simplex Cubature Rule

For nonlinear systems, as shown in (2) and (4), the posterior mean value cannot be propagated directly using the nonlinear function, and it results in the crucial problem in nonlinear Kalman filter being the calculation of the integral of the form “nonlinear function \times Gaussian PDF”. Specifically, that is to calculate the integral $I_N = \int_{\mathbf{R}^n} \mathbf{g}(\mathbf{x}) N(\mathbf{x}; \widehat{\mathbf{x}}, \mathbf{P}_x) d\mathbf{x}$, where $\mathbf{x} \in \mathbf{R}^n$, $\mathbf{g}(\mathbf{x})$ denotes the arbitrary nonlinear function, and $N(\mathbf{x}; \widehat{\mathbf{x}}, \mathbf{P}_x)$ represents the Gaussian distribution with mean $\widehat{\mathbf{x}}$ and covariance \mathbf{P}_x . Owing to it being difficult to achieve the analytical solution, finding the high accuracy integral rule for numerical approximation becomes momentous, and the cubature rule is taken into account in this section.

3.1. Spherical Simplex Rule for Spherical Integral. The integral of the form $I_g = \int_{\mathbf{R}^n} \mathbf{g}(\mathbf{x}) \exp(-\mathbf{x}^T \mathbf{x}) d\mathbf{x}$ is considered first, and it needs to be transformed into the spherical-radial coordinate system to compute the integral I_g numerically. For this purpose, let $\mathbf{x} = r\mathbf{s}$, where $\mathbf{s} = (s_1, s_2, \dots, s_n)^T$ represents the direction vector such that $\mathbf{s}^T \mathbf{s} = 1$ and $r = \sqrt{\mathbf{x}^T \mathbf{x}} \in [0, \infty)$ denotes the radius. Then the integral I_g can be decomposed into the spherical integral $S(r)$ and the radial integral R as follows [10], which are easier to approximate numerically compared with I_g .

$$S(r) = \int_{U_n} \mathbf{g}(r\mathbf{s}) d\sigma(\mathbf{s}) \quad (5)$$

$$R = \int_0^\infty S(r) r^{n-1} \exp(-r^2) dr \quad (6)$$

where $U_n = \{\mathbf{s} \in \mathbf{R}^n : s_1^2 + s_2^2 + \dots + s_n^2 = 1\}$ denotes the spherical surface, and $d\sigma(\cdot)$ represents the area element on U_n .

The spherical integral $S(r)$ is approximated using the following third-order spherical simplex rule consisting of $2n+2$ points [14].

$$S(r) \approx \frac{T_n}{2(n+1)} \sum_{i=1}^{n+1} [\mathbf{g}(r\mathbf{a}_i) + \mathbf{g}(-r\mathbf{a}_i)] \quad (7)$$

where $T_n = 2\sqrt{\pi^n}/\Gamma(n/2)$ denotes the surface area of the unit sphere and $\Gamma(x) = \int_0^\infty \exp(-t)t^{x-1}dt$ is the Gamma function. The vectors $\mathbf{a}_i = (a_{i,1}, a_{i,2}, \dots, a_{i,n})^\top$, $i = 1, 2, \dots, n+1$ are the vertices of the n -dimensional simplex, and the elements are defined as follows.

$$a_{i,j} = \begin{cases} -\sqrt{\frac{n+1}{n(n-j+2)(n-j+1)}}, & j < i \\ \sqrt{\frac{(n+1)(n-i+1)}{n(n-i+2)}}, & i = j \\ 0, & j > i \end{cases} \quad (8)$$

3.2. Generalized Gauss-Laguerre Quadrature Rule for Radial Integral. As for the radial integral $R = \int_0^\infty S(r)r^{n-1}\exp(-r^2)dr$, we need to transform it into the standard form. For this, let $r = \sqrt{t}$ and $R = (1/2)\int_0^\infty S(\sqrt{t})t^{n/2-1}\exp(-t)dt$ is deduced. Further, let $\tilde{S}(t) = S(\sqrt{t})$ and $\beta = n/2 - 1$, then R is written in the form of $R = (1/2)\int_0^\infty \tilde{S}(t)t^\beta \exp(-t)dt$, which is approximated numerically using the following generalized Gauss-Laguerre quadrature rule [15].

$$\int_0^\infty \tilde{S}(t)t^\beta \exp(-t)dt \approx \sum_{i=1}^p \tilde{\omega}_i \tilde{S}(t_i) \quad (9)$$

where t_i and $\tilde{\omega}_i$ represent the quadrature points and the corresponding weights, respectively. p denotes the number of the points. Points t_i can be obtained by solving the following m -order Chebyshev-Laguerre polynomials.

$$L_p^\beta(t) = (-1)^p t^{-\beta} \exp(t) \frac{d^p}{dt^p} (t^{\beta+p} \exp(-t)) = 0 \quad (10)$$

Weights $\tilde{\omega}_i$ are calculated using the following:

$$\tilde{\omega}_i = \frac{p!\Gamma(\beta+p+1)}{t_i [L_p^\beta(t_i)]^2} \quad (11)$$

3.3. Simplex Cubature Rule for Approximation. Through substituting (7) and $\tilde{S}(t) = S(\sqrt{t})$ into (9), the radial integral R is written as follows:

$$\begin{aligned} R &= \frac{1}{2} \int_0^\infty \tilde{S}(t)t^\beta \exp(-t)dt \approx \frac{1}{2} \sum_{j=1}^p \tilde{\omega}_j S(\sqrt{t_j}) \\ &= \frac{T_n}{4(n+1)} \sum_{j=1}^p \tilde{\omega}_j \sum_{i=1}^{n+1} [\mathbf{g}(\sqrt{t_j}\mathbf{a}_i) + \mathbf{g}(-\sqrt{t_j}\mathbf{a}_i)] \\ &= \frac{\sqrt{\pi^n}}{2(n+1)\Gamma(n/2)} \\ &\quad \cdot \sum_{j=1}^p \tilde{\omega}_j \sum_{i=1}^{n+1} [\mathbf{g}(\sqrt{t_j}\mathbf{a}_i) + \mathbf{g}(-\sqrt{t_j}\mathbf{a}_i)] \end{aligned} \quad (12)$$

It can be proved that I_N has the following equivalent form:

$$I_N = \frac{1}{\sqrt{\pi^n}} \int_{\mathbf{R}^n} \mathbf{g}(\sqrt{2\mathbf{P}_x \mathbf{x} + \hat{\mathbf{x}}}) \exp(-\mathbf{x}^\top \mathbf{x}) d\mathbf{x} \quad (13)$$

Combined with (13), we achieve the following generalized simplex cubature rule to approximate the nonlinear Gaussian weighted integral.

$$\begin{aligned} I_N &\approx \frac{1}{2(n+1)\Gamma(n/2)} \sum_{j=1}^p \tilde{\omega}_j \sum_{i=1}^{n+1} [\mathbf{g}(\sqrt{2t_j\mathbf{P}_x \mathbf{a}_i + \hat{\mathbf{x}}}) \\ &\quad + \mathbf{g}(-\sqrt{2t_j\mathbf{P}_x \mathbf{a}_i + \hat{\mathbf{x}}})] \end{aligned} \quad (14)$$

It can be seen from (14) that $2(n+1)p$ points with corresponding weights are needed. For $p \geq 3$, the difficulty in finding a general expression between n and $t_i, \tilde{\omega}_i$ will bring some trouble; meanwhile, with the third-order spherical simplex rule, the improvement in accuracy caused by the higher-order Gauss-Laguerre quadrature rule is limited in practical applications. Hence, we choose $p = 2$, and (10) and (11) turn into the following forms, respectively.

$$L_2^\beta(t) = t^{-\beta} \exp(t) \frac{d^2}{dt^2} (t^{\beta+2} e^{-t}) = 0 \quad (15)$$

$$\tilde{\omega}_i = \frac{2\Gamma(\beta+3)}{t_i [L_2^\beta(t_i)]^2} \quad (16)$$

The solutions of $t_1, t_2, \tilde{\omega}_1, \tilde{\omega}_2$ can be solved from (15) and (16) as follows:

$$\begin{aligned} t_1 &= \frac{n}{2} + 1 + \sqrt{\frac{n}{2} + 1} \\ t_2 &= \frac{n}{2} + 1 - \sqrt{\frac{n}{2} + 1}, \end{aligned} \quad (17)$$

$$\tilde{\omega}_1 = \frac{n\Gamma(n/2)}{2n+4+2\sqrt{2n+4}}$$

$$\tilde{\omega}_2 = \frac{n\Gamma(n/2)}{2n+4-2\sqrt{2n+4}}$$

The new simplex cubature rule is derived by substituting (17) into (14) as follows:

$$I_N \approx \frac{n}{4(n+1)(n+2+\sqrt{2n+4})} \cdot \sum_{i=1}^{n+1} \left[\mathbf{g} \left(\hat{\mathbf{x}} + \sqrt{(n+2+\sqrt{2n+4})} \mathbf{P}_x \mathbf{a}_i \right) + \mathbf{g} \left(\hat{\mathbf{x}} - \sqrt{(n+2+\sqrt{2n+4})} \mathbf{P}_x \mathbf{a}_i \right) \right]$$

$$+ \frac{n}{4(n+1)(n+2-\sqrt{2n+4})} \times \sum_{i=1}^{n+1} \left[\mathbf{g} \left(\hat{\mathbf{x}} + \sqrt{(n+2-\sqrt{2n+4})} \mathbf{P}_x \mathbf{a}_i \right) + \mathbf{g} \left(\hat{\mathbf{x}} - \sqrt{(n+2-\sqrt{2n+4})} \mathbf{P}_x \mathbf{a}_i \right) \right] = \sum_{i=1}^{4n+4} \omega_i \mathbf{g} \left(\hat{\mathbf{x}}^{(i)} \right) \quad (18)$$

The above rule consists of $4(n+1)$ points, and the cubature points $\hat{\mathbf{x}}^{(i)}$ and weights ω_i in (18) are given as follows:

$$\hat{\mathbf{x}}^{(i)} = \begin{cases} \hat{\mathbf{x}} + \sqrt{(n+2+\sqrt{2n+4})} \mathbf{P}_x [\mathbf{a}, -\mathbf{a}]_i, & i = 1, 2, \dots, 2n+2 \\ \hat{\mathbf{x}} + \sqrt{(n+2-\sqrt{2n+4})} \mathbf{P}_x [\mathbf{a}, -\mathbf{a}]_{i-2n-2}, & i = 2n+3, \dots, 4n+4 \end{cases} \quad (19)$$

$$\omega_i = \begin{cases} \frac{n}{4(n+1)(n+2+\sqrt{2n+4})}, & i = 1, 2, \dots, 2n+2 \\ \frac{n}{4(n+1)(n+2-\sqrt{2n+4})}, & i = 2n+3, \dots, 4n+4 \end{cases} \quad (20)$$

where matrix $\mathbf{a} = [\mathbf{a}_1, \mathbf{a}_2, \dots, \mathbf{a}_{n+1}]$ and $[\cdot]_i$ indicates the i -th column of the matrix. Take $n = 3$ for example; \mathbf{a} is the matrix given as follows.

$$\begin{bmatrix} 1 & -\frac{1}{3} & -\frac{1}{3} & -\frac{1}{3} \\ 0 & \frac{\sqrt{8}}{3} & -\frac{\sqrt{2}}{3} & -\frac{\sqrt{2}}{3} \\ 0 & 0 & \frac{\sqrt{6}}{3} & -\frac{\sqrt{6}}{3} \end{bmatrix} \quad (21)$$

4. Distributed Simplex Cubature Kalman-Consensus Filter

The centralized method and the distributed one in the space target tracking using multiple radars are generally illustrated in Figures 2(a) and 2(b), respectively. It is obvious that the main difference of these two methods is the existence of the fusion center, which decides the information fusion mode. Suppose the radars in Figure 2(b) are in a wireless network, and if a message is transmitted between two radars, we use s to denote the sending radar and c to denote the receiving and calculating radar. The radars that have the ability to communicate with the radar c are defined as its neighbor radars, which are denoted as N_c , and the set $J_c = N_c \cup c$ represents N_c with the radar c itself included. Here, the following two assumptions are given as in [20].

(1) The radars have the ability to communicate with each other, and the links are stable and reliable.

(2) The information can be transmitted and processed within one filter cycle.

The state equation and the measurement equation, which are given in (2) and (4), respectively, are rewritten in the general nonlinear forms, and the following nonlinear system is taken into account.

$$\begin{aligned} \mathbf{x}_{c,k} &= \mathbf{f}(\mathbf{x}_{c,k-1}) + \mathbf{w}_{c,k} \\ \mathbf{z}_{c,k} &= \mathbf{h}_c(\mathbf{x}_{c,k}) + \mathbf{v}_{c,k} \end{aligned} \quad (22)$$

where c denotes the models running on the radar c . $\mathbf{x}_{c,k} \in \mathbf{R}^n$ and $\mathbf{z}_{c,k} \in \mathbf{R}^q$ are the state and measurement vectors, respectively, while $\mathbf{w}_{c,k}$ and $\mathbf{v}_{c,k}$ denote the white Gaussian noise with the covariance being $\mathbf{Q}_{c,k}$ and $\mathbf{R}_{c,k}$, respectively.

For linear system, the measurement model in (22) reduces to $\mathbf{z}_{c,k} = \mathbf{H}_c \mathbf{x}_{c,k} + \mathbf{v}_{c,k}$, where \mathbf{H}_c denotes the measurement matrix. The information vector and matrix that exchanged among the neighbor radars are defined using the measurement matrix \mathbf{H}_c in the Kalman-consensus filter [21]. Hence, for nonlinear system, the nonlinear function $\mathbf{z}_{c,k} = \mathbf{h}_c(\mathbf{x}_{c,k}) + \mathbf{v}_{c,k}$ needs to be linearized to find the equivalent expression of \mathbf{H}_c , and the proposed simplex cubature rule should be introduced to improve the filtering accuracy without derivation.

The statistical linear regression method is adopted, and the resulting linearized function is more accurate in a statistical sense than simply using a first-order truncated Taylor series [25]. For clarity, the subscripts are omitted in the absence of ambiguity, and the objective is to find the linear estimator of $\mathbf{z} = \mathbf{h}(\mathbf{x}) + \mathbf{v}$, such that $\hat{\mathbf{z}} = \mathbf{H}\mathbf{x} + \mathbf{b} + \mathbf{v}$. The matrix

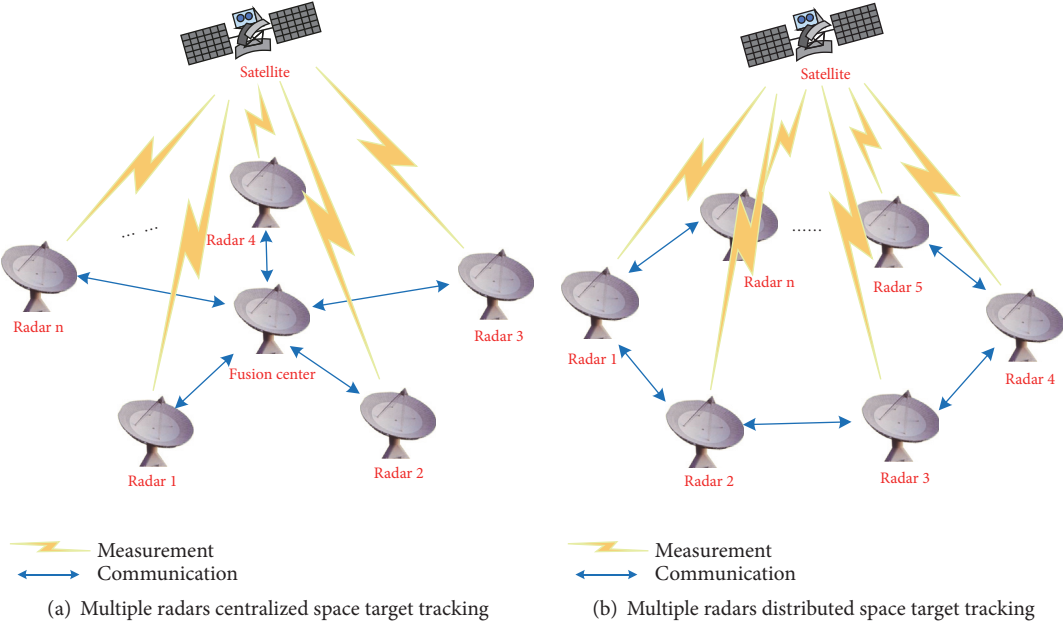


FIGURE 2: Multiple radar space target tracking.

\mathbf{H} and vector \mathbf{b} are determined by minimizing the criterion function $\{\mathbf{H}, \mathbf{b}\} = \arg \min \mathbb{E}\{\|\mathbf{h}(\mathbf{x}) - \mathbf{H}\mathbf{x} - \mathbf{b}\|_2^2\}$, through the partial derivative with respect to \mathbf{b} to zero and the gradient with respect to \mathbf{A} to zero, respectively, we obtain $\mathbf{H} = \mathbf{P}_{xz}^T \mathbf{P}^{-1}$, where \mathbf{P}_{xz} denotes the cross covariance, and \mathbf{P} represents the covariance of \mathbf{x} .

By means of the proposed simplex cubature rule and the equation $\mathbf{H}_{c,k} = \mathbf{P}_{c,xz,k}^T (\mathbf{P}_{c,k}^-)^{-1}$ (with the subscript), the proposed SCKCF is derived based on the KCF framework, and the specific calculation steps are given below.

Step 1 (filter initialization). Give the initial filter values $\hat{\mathbf{x}}_{c,0}^+$ and $\mathbf{P}_{c,0}^+$. Cycle $k = 1, 2, \dots$, and finish the following steps.

Step 2 (time update). The posterior state $\hat{\mathbf{x}}_{c,k-1}^+$ and covariance $\mathbf{P}_{c,k-1}^+$ at time $k - 1$ are used instead of $\hat{\mathbf{x}}$ and \mathbf{P}_x in (19), respectively, to calculate the cubature points $\hat{\mathbf{x}}_{c,k-1}^{(i)}$, which are propagated by nonlinear function $\mathbf{f}(\cdot)$ as follows.

$$\mathbf{X}_{c,k}^{(i)} = \mathbf{f}(\hat{\mathbf{x}}_{c,k-1}^{(i)}) \quad (23)$$

The prior state estimate $\hat{\mathbf{x}}_{c,k}^-$ and the covariance $\mathbf{P}_{c,k}^-$ are calculated using the propagated points $\mathbf{X}_{c,k}^{(i)}$ and weights ω_i , where ω_i are given in (20).

$$\hat{\mathbf{x}}_{c,k}^- = \sum_{i=1}^{4n+4} \omega_i \mathbf{X}_{c,k}^{(i)} \quad (24)$$

$$\mathbf{P}_{c,k}^- = \sum_{i=1}^{4n+4} \omega_i (\mathbf{X}_{c,k}^{(i)} - \hat{\mathbf{x}}_{c,k}^-) (\mathbf{X}_{c,k}^{(i)} - \hat{\mathbf{x}}_{c,k}^-)^T + \mathbf{Q}_{c,k} \quad (25)$$

Step 3 (measurement update). The prior state $\hat{\mathbf{x}}_{c,k}^-$ and covariance $\mathbf{P}_{c,k}^-$ at time k are used instead of $\hat{\mathbf{x}}$ and \mathbf{P}_x in (19), respectively, to calculate the cubature points $\hat{\mathbf{x}}_{c,k}^{(i)}$, which are propagated by nonlinear function $\mathbf{h}_c(\cdot)$ as follows.

$$\mathbf{Z}_{c,k}^{(i)} = \mathbf{h}_c(\hat{\mathbf{x}}_{c,k}^{(i)}) \quad (26)$$

The predicted measurement $\hat{\mathbf{z}}_{c,k}$ and cross covariance $\mathbf{P}_{c,xz,k}$ are approximated using the propagated points $\mathbf{Z}_{c,k}^{(i)}$ and weights ω_i , where ω_i are given in (20).

$$\hat{\mathbf{z}}_{c,k} = \sum_{i=1}^{4n+4} \omega_i \mathbf{Z}_{c,k}^{(i)} \quad (27)$$

$$\mathbf{P}_{c,xz,k} = \sum_{i=1}^{2n+2} \omega_i (\hat{\mathbf{x}}_{c,k}^{(i)} - \hat{\mathbf{x}}_{c,k}^-) (\mathbf{Z}_{c,k}^{(i)} - \hat{\mathbf{z}}_{c,k})^T \quad (28)$$

Compute the information vector and matrix of the sending radar:

$$\mathbf{u}_{c,k} = \mathbf{H}_{c,k}^T \mathbf{R}_{c,k}^{-1} \boldsymbol{\varepsilon}_{c,k} = (\mathbf{P}_{c,k}^-)^{-1} \mathbf{P}_{c,xz,k} \mathbf{R}_{c,k}^{-1} \boldsymbol{\varepsilon}_{c,k} \quad (29)$$

$$\begin{aligned} \mathbf{U}_{c,k} &= \mathbf{H}_{c,k}^T \mathbf{R}_{c,k}^{-1} \mathbf{H}_{c,k} \\ &= (\mathbf{P}_{c,k}^-)^{-1} \mathbf{P}_{c,xz,k} \mathbf{R}_{c,k}^{-1} \mathbf{P}_{c,xz,k}^T (\mathbf{P}_{c,k}^-)^{-1} \end{aligned} \quad (30)$$

where $\boldsymbol{\varepsilon}_{c,k} = \mathbf{z}_{c,k} - \hat{\mathbf{z}}_{c,k}$ denotes the residual.

Step 4 (broadcast and receive message). The message $\mathbf{m}_{c,k} = (\mathbf{u}_{c,k}, \mathbf{U}_{c,k}, \hat{\mathbf{x}}_{c,k}^-)$ is broadcasted to the neighbor radars, meanwhile receiving the same defined messages $\mathbf{m}_{s,k} = (\mathbf{u}_{s,k}, \mathbf{U}_{s,k}, \hat{\mathbf{x}}_{s,k}^-)$ from its neighbors.

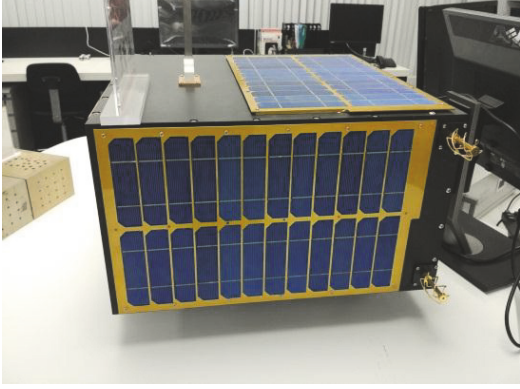


FIGURE 3: Space target simulator.

Step 5 (information fusion). The received messages are fused to obtain matrix $\mathbf{S}_{c,k}$ and vector $\mathbf{g}_{c,k}$.

$$\mathbf{S}_{c,k} = \sum_{s \in \mathcal{J}_c} \mathbf{U}_{s,k} \quad (31)$$

$$\mathbf{g}_{c,k} = \sum_{s \in \mathcal{J}_c} (\mathbf{u}_{s,k} - \mathbf{U}_{s,k} (\hat{\mathbf{x}}_{c,k}^- - \hat{\mathbf{x}}_{s,k}^-)) \quad (32)$$

Step 6 (state update). The posterior covariance $\mathbf{P}_{c,k}^+$ and state estimate $\hat{\mathbf{x}}_{c,k}^+$ are calculated.

$$\mathbf{P}_{c,k}^+ = \left[(\mathbf{P}_{c,k}^-)^{-1} + \mathbf{S}_{c,k} \right]^{-1} \quad (33)$$

$$\hat{\mathbf{x}}_{c,k}^+ = \hat{\mathbf{x}}_{c,k}^- + \mathbf{P}_{c,k}^+ \mathbf{g}_{c,k} + \gamma \mathbf{P}_{c,k}^- \sum_{s \in \mathcal{N}_c} (\hat{\mathbf{x}}_{s,k}^- - \hat{\mathbf{x}}_{c,k}^-) \quad (34)$$

where $\gamma = \alpha / (1 + \|\mathbf{P}_{c,k}^-\|_F)$, α is a small constant, and $\|\cdot\|_F$ is the Frobenius norm of the matrix.

By means of the information exchange among the neighbor radars, the estimate of each radar, that is, $\hat{\mathbf{x}}_{c,k}^+$, can reach a asymptotical consensus through the above distributed filter [21].

5. Simulation Results and Analysis

A space target tracking simulation is given in this section to show the performance of the proposed SCKCF. The space target simulator, which runs the high-precision orbit propagation algorithm and provides the orbit simulation data, is shown in Figure 3. The perturbations, mainly including the high-order nonspherical gravitational perturbation, the atmospheric drag, the solar radiation pressure, the three-body gravity, and the tide perturbation, are taken into account, where the atmospheric drag coefficient $c_d = 2.2$, and the area-to-mass ratio of satellite is $0.02 \text{ m}^2/\text{kg}$. Furthermore, the Jacchia-Roberts model is used as the atmospheric density model and the solar radiation pressure coefficient $c_r = 1$. The space target runs in sun-synchronous low earth orbit, the orbit epoch is 1 July, 2016, 12:00:00 (UTC), and the six orbit elements are $a = 6978.14 \text{ km}$, $e = 0$, $i = 97.79^\circ$, $\Omega = 279.76^\circ$, $\omega = 0^\circ$, and $f = 0^\circ$, respectively.

The latitudes and longitudes as well as the communication topology of the six radars are shown in Figure 4. The measurement errors of the range, velocity, and the angles are 60 m , 0.1 m/s , and 0.02° , respectively. The minimum elevation angle is 10° , and the access time between the space target and all the radars is from 04:41:50 to 04:48:00 on 2 July, 2016, for a total of 370s. As shown in Figure 4, each radar only exchanges information with its two neighbor radars, so there is no information fusion center in the system and the failures of any one cannot result in the collapse of the space target tracking system.

In this simulation, the proposed SCKCF is compared with the CKF performed by single radar, the cubature Kalman-consensus filter (CKCF), and the centralized filter. The parameter $\alpha = 0.01$, the initial filter state $\hat{\mathbf{x}}_{c,0}^+$, and the initial covariance matrix $\mathbf{P}_{c,0}^+$ are given as follows:

$$\hat{\mathbf{x}}_{c,0}^+ = (-1485607, 4323895, 5272734, -327, 5803, -4830)^T \quad (35)$$

$$\mathbf{P}_{c,0}^+ = \text{diag}(1000^2, 1000^2, 1000^2, 10^2, 10^2, 10^2)$$

The covariances $\mathbf{Q}_{c,k}$ and $\mathbf{R}_{c,k}$ are given as follows:

$$\mathbf{Q}_{c,k} = \text{diag}(0.001^2, 0.001^2, 0.001^2, 0.00001^2, 0.00001^2, 0.00001^2) \quad (36)$$

$$\mathbf{R}_{c,k} = \text{diag}\left(60^2, 0.1^2, \left(\frac{0.02\pi}{180}\right)^2, \left(\frac{0.02\pi}{180}\right)^2\right)$$

The filtering interval is 1s, that means the data should be collected and processed in 1s. The metrics used to compare the space target tracking accuracy of various filters is the root mean square error (RMSE). The Monte Carlo simulation is conducted 200 times, and the RMSEs of the position and velocity are shown in Figures 5–10. The logarithmic scale is used on the y-axis in order to improve the readability. From the figures, we can see that the RMSEs of the CKCF and the proposed SCKCF are significant smaller than that of the CKF performed by single radar, indicating that the multiple radars information fusion could obtain higher space target tracking accuracy. Moreover, the RMSEs of the centralized filter are the smallest, indicating that the distributed filters could acquire the suboptimal estimates compared with the centralized one.

The mean RMSEs from 200s to 370s are calculated and summarized in Tables 1 and 2. As shown in the figures, the CKF and the centralized filter achieve the worst and best accuracy, respectively. As for the two distributed filters, the proposed SCKCF achieves more accurate results compared with the CKCF, because SCKCF adopts the proposed simplex cubature rule while the CKCF adopts the conventional cubature rule. In the new simplex cubature rule, the spherical integral and radial integral are calculated using the spherical simplex rule and second-order Gauss-Laguerre quadrature rule, respectively; that is, two points are used in the radial integral while only one point is used in that of the conventional cubature rule, and the spherical simplex rule has

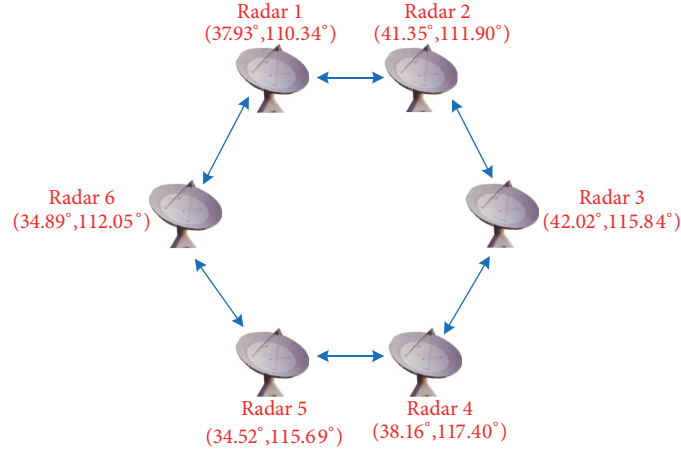


FIGURE 4: Locations and communication topology.

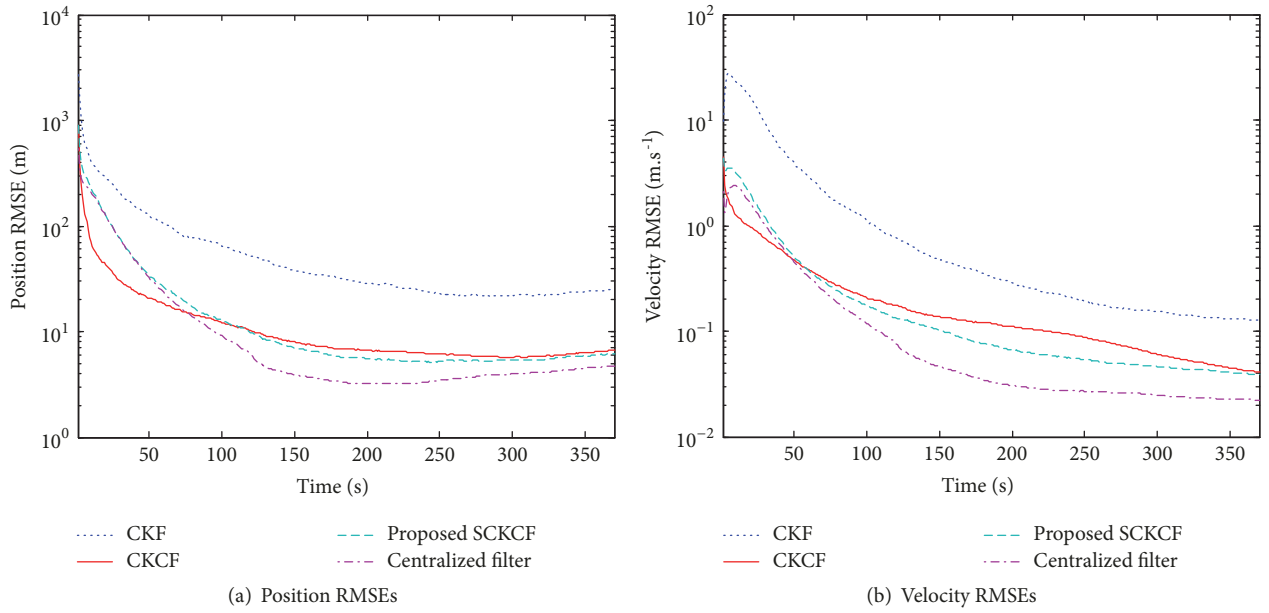


FIGURE 5: RMSEs of the space target tracking of radar 1.

TABLE 1: Mean position RMSEs.

Filters	Radar 1/m	Radar 2/m	Radar 3/m	Radar 4/m	Radar 5/m	Radar 6/m
CKF	23.7473	35.4105	37.2135	23.8687	21.1308	17.2393
CKCF	6.1371	6.6633	6.9016	6.8462	6.6887	6.7597
Proposed SCKCF	5.4843	5.3668	5.1280	4.6526	4.3772	4.4636
Centralized filter	3.8374					

TABLE 2: Mean velocity RMSEs.

Filters	Radar 1 /(m·s ⁻¹)	Radar 2 /(m·s ⁻¹)	Radar 3 /(m·s ⁻¹)	Radar 4 /(m·s ⁻¹)	Radar 5 /(m·s ⁻¹)	Radar 6 /(m·s ⁻¹)
CKF	0.1750	0.2317	0.2317	0.1801	0.2077	0.1999
CKCF	0.0713	0.0433	0.0411	0.0449	0.0397	0.0439
Proposed SCKCF	0.0496	0.0343	0.0317	0.0334	0.0342	0.0339
Centralized filter	0.0256					

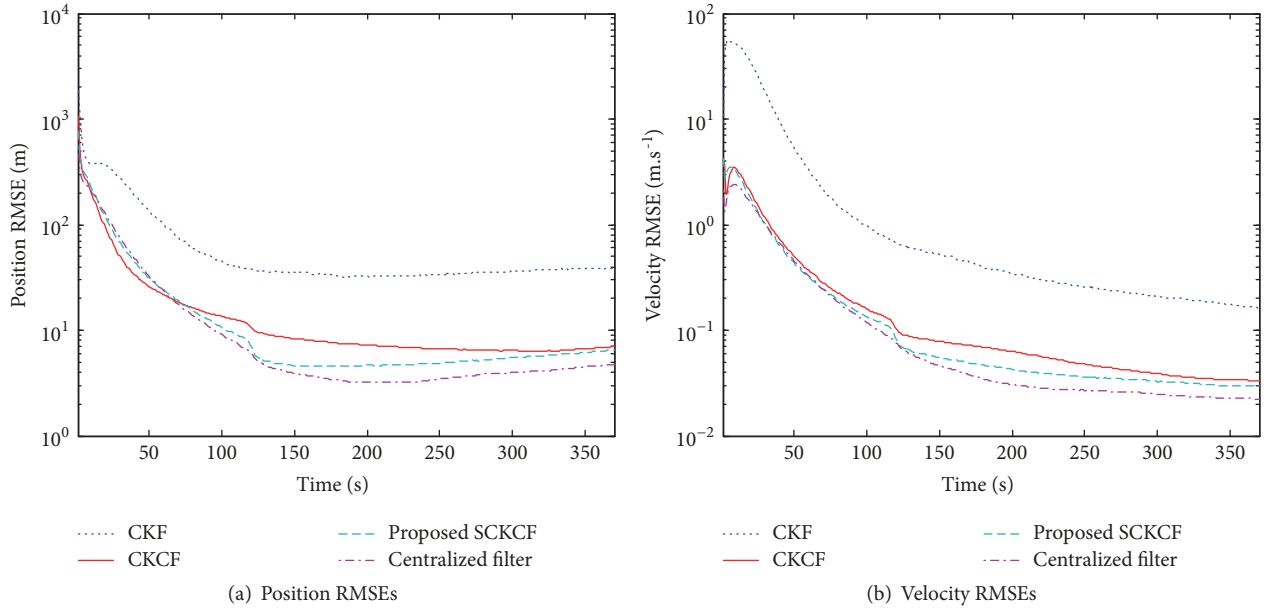


FIGURE 6: RMSEs of the space target tracking of radar 2.

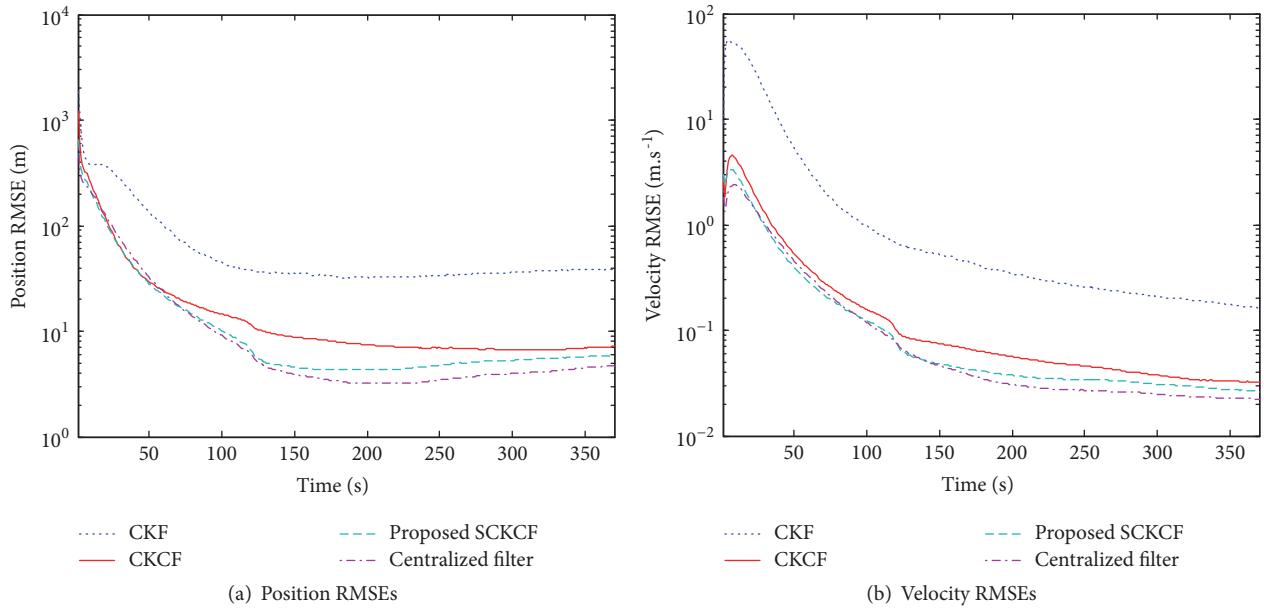


FIGURE 7: RMSEs of the space target tracking of radar 3.

better performance than spherical rule in this application; thus the proposed simplex cubature rule outperforms in approximating the nonlinear orbital states.

6. Conclusions

To improve the distributed space target tracking accuracy by multiple radars, a simplex cubature Kalman-consensus filter is proposed in this paper. The intractable integral is

approximated using a new simplex cubature rule, which is more accurate compared with the traditional cubature rule. By means of the statistical linear regression method, the posterior mean, covariance, and the transmitted messages in the Kalman-consensus filter are approximated using the deduced simplex cubature rule, which results in the proposed SCKCF. There is no data fusion center in the filter, and each radar needs to exchange the information only with its neighbors to reach a consensus estimate. The simulation results show that the proposed SCKCF can achieve more

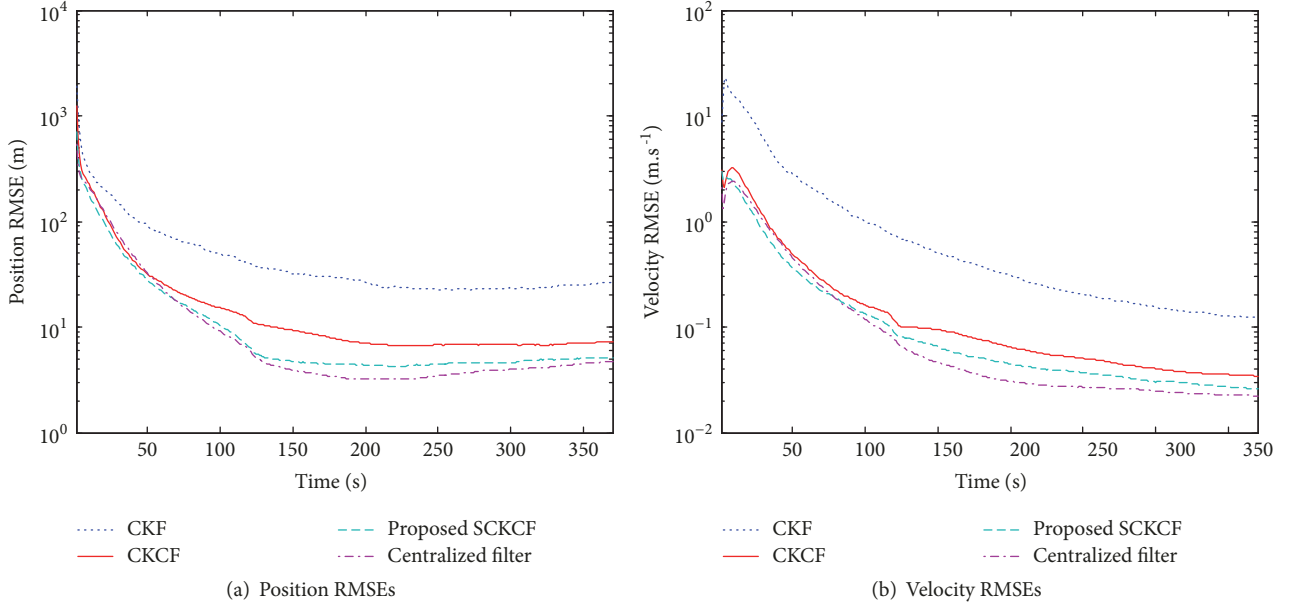


FIGURE 8: RMSEs of the space target tracking of radar 4.

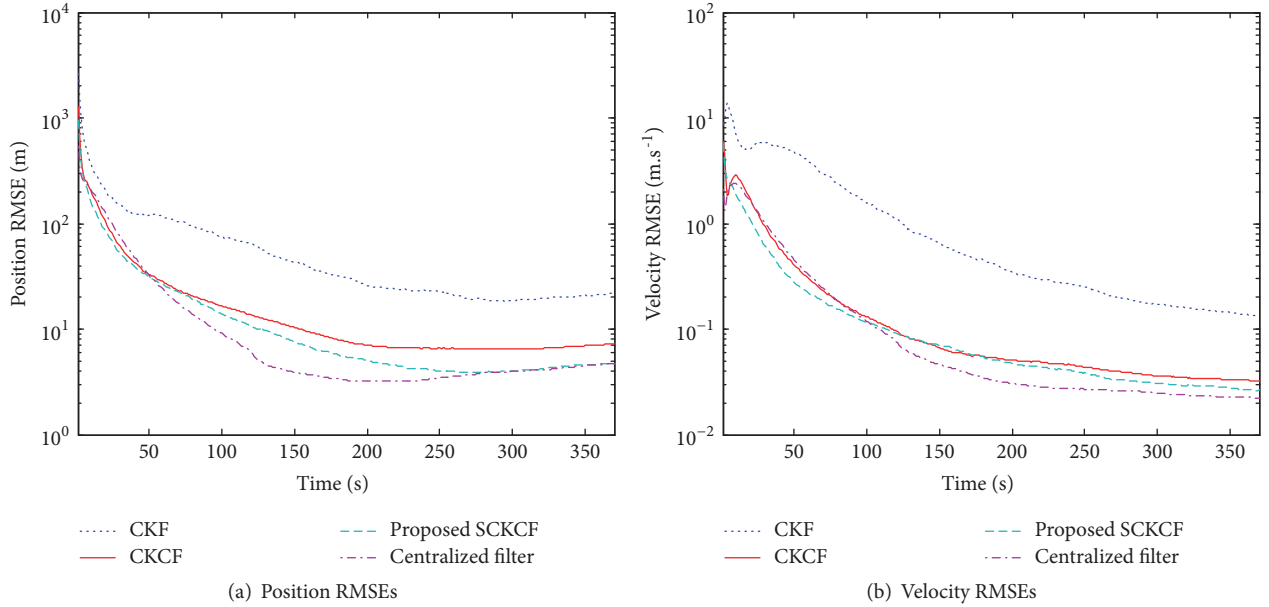


FIGURE 9: RMSEs of the space target tracking of radar 5.

accurate results compared with the CKCF, thus verifying the validity of the proposed filter. The neighboring radars are required to communicate mutually in the proposed SCKCF. However, if the link between the radars can be simplified to one-way mode without reducing accuracy, that is, the communication topology is described using the directed graph instead of the undirected graph, it can further reduce the communication burden to a certain extent. Therefore, more advanced consensus algorithms should

be investigated and combined with the CKF in the next study.

Appendix

The detailed process of the coordinate transformation from $O - XYZ$ to $O - X_h Y_h Z_h$ is given as follows.

The transformation is performed in two steps, and the WGS84 earth fixed coordinate system ($O - X_e Y_e Z_e$, the red

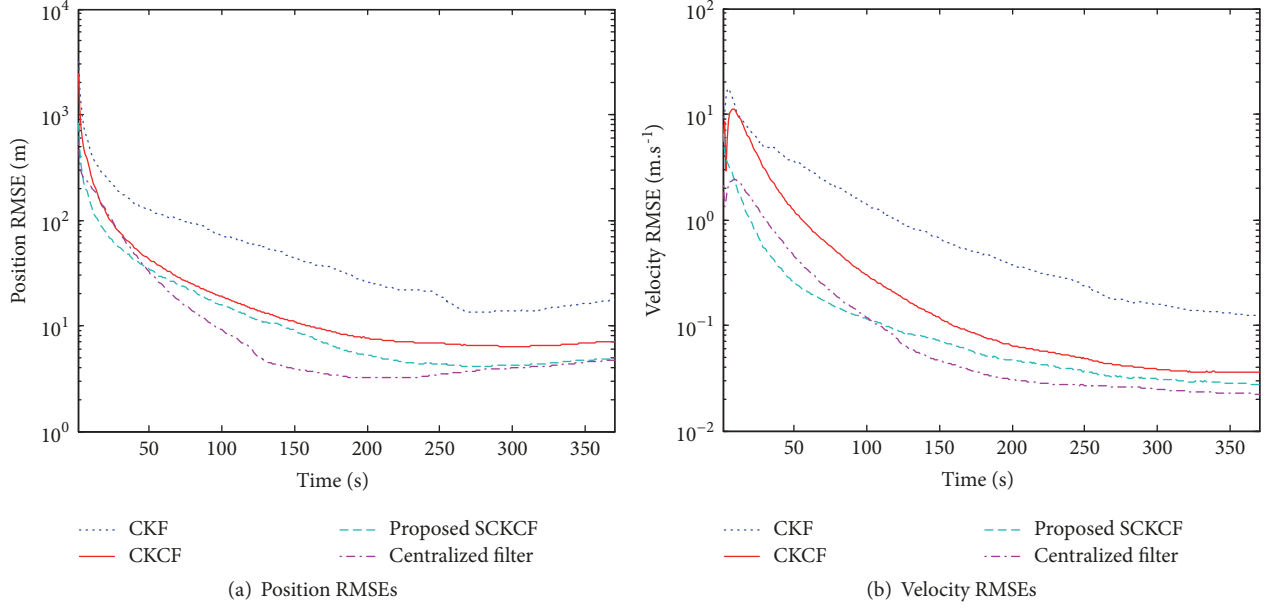


FIGURE 10: RMSEs of the space target tracking of radar 6.

one in Figure 2) should be used. The orbital state in $O - X_e Y_e Z_e$ is expressed as $\tilde{\mathbf{X}}_k = (\tilde{\mathbf{X}}_{p,k}^T, \tilde{\mathbf{X}}_{v,k}^T)^T$.

Step 1 (Transformation from $O - XYZ$ to $O - X_e Y_e Z_e$). The coordinate transformation is given as follows:

$$\begin{bmatrix} \tilde{\mathbf{X}}_{p,k} \\ \tilde{\mathbf{X}}_{v,k} \end{bmatrix} = \begin{bmatrix} \mathbf{M}_J^W & \mathbf{0} \\ \dot{\mathbf{M}}_J^W & \mathbf{M}_J^W \end{bmatrix} \begin{bmatrix} \mathbf{X}_{p,k} \\ \mathbf{X}_{v,k} \end{bmatrix} \quad (\text{A.1})$$

where $\mathbf{M}_J^W = \mathbf{M}_{Pw} \mathbf{M}_{Ro} \mathbf{M}_{Nu} \mathbf{M}_{Pr}$ denotes the transfer matrix, and \mathbf{M}_{Pr} , \mathbf{M}_{Nu} , \mathbf{M}_{Ro} , \mathbf{M}_{Pw} represent the precession matrix, the nutation matrix, the rotation matrix, and the polar shift matrix, respectively. The derivative matrix $\dot{\mathbf{M}}_J^W \approx \mathbf{M}_{Pw} (d(\mathbf{M}_{Ro})/dt) \mathbf{M}_{Nu} \mathbf{M}_{Pr}$, and $d(\mathbf{M}_{Ro})/dt$ is given as follows:

$$\frac{d(\mathbf{M}_{Ro})}{dt} = \begin{bmatrix} 0 & \omega_e & 0 \\ -\omega_e & 0 & 0 \\ 0 & 0 & 0 \end{bmatrix} \cdot \mathbf{M}_{Ro} \quad (\text{A.2})$$

where ω_e is the rotational angular velocity of the earth.

Step 2 (Transformation from $O - X_e Y_e Z_e$ to $O - X_h Y_h Z_h$). The coordinate transformation is given as follows:

$$\begin{bmatrix} \hat{\mathbf{X}}_{p,k} \\ \hat{\mathbf{X}}_{v,k} \end{bmatrix} = \begin{bmatrix} \mathbf{M}_W^H & \mathbf{0} \\ \mathbf{0} & \mathbf{M}_W^H \end{bmatrix} \begin{bmatrix} \tilde{\mathbf{X}}_{p,k} \\ \tilde{\mathbf{X}}_{v,k} \end{bmatrix} - \begin{bmatrix} \mathbf{M}_W^H \mathbf{Y}_{c,k} \\ \mathbf{0} \end{bmatrix} \quad (\text{A.3})$$

where the matrix \mathbf{M}_W^H is given as follows:

$$\mathbf{M}_W^H = \begin{bmatrix} -\sin \lambda & \cos \lambda & 0 \\ -\sin \varphi \cos \lambda & -\sin \varphi \sin \lambda & \cos \varphi \\ \cos \varphi \cos \lambda & \cos \varphi \sin \lambda & \sin \varphi \end{bmatrix} \quad (\text{A.4})$$

where λ and φ represent the geocentric longitude and latitude of the radar, respectively, which can be changed into the geocentric coordinate \mathbf{Y}_c of this radar in $O - X_e Y_e Z_e$.

Consequently, by substituting (A.1) into (A.3), we achieve the following coordinate transformation from $O - XYZ$ to $O - X_h Y_h Z_h$.

$$\begin{bmatrix} \hat{\mathbf{X}}_{p,k} \\ \hat{\mathbf{X}}_{v,k} \end{bmatrix} = \begin{bmatrix} \mathbf{M}_W^H & \mathbf{0} \\ \mathbf{0} & \mathbf{M}_W^H \end{bmatrix} \begin{bmatrix} \mathbf{M}_J^W & \mathbf{0} \\ \dot{\mathbf{M}}_J^W & \mathbf{M}_J^W \end{bmatrix} \begin{bmatrix} \mathbf{X}_{p,k} \\ \mathbf{X}_{v,k} \end{bmatrix} - \begin{bmatrix} \mathbf{M}_W^H \mathbf{Y}_c \\ \mathbf{0} \end{bmatrix} \quad (\text{A.5})$$

Data Availability

The data used to support the findings of this study are available from the corresponding author upon request.

Conflicts of Interest

The authors declare that they have no conflicts of interest.

Acknowledgments

This work is supported by the National High Technology Research and Development Program of China under Grant 2015AA7026085.

References

- [1] A. K. Singh and S. Bhaumik, "Tracking of low earth orbit satellite using cubature quadrature Kalman filter," in *Proceedings of the IEEE International Symposium on Signal Processing and Information Technology*, pp. 114–118, Noida, India, 2014.

- [2] F. Daum, "Nonlinear filters: beyond the Kalman filter," *IEEE Aerospace and Electronic Systems Magazine*, vol. 20, no. 8, pp. 57–69, 2005.
- [3] A. Doucet, S. Godsill, and C. Andrieu, "On sequential Monte Carlo sampling methods for Bayesian filtering," *Statistics and Computing*, vol. 10, no. 3, pp. 197–208, 2000.
- [4] S. Y. Wang, J. C. Feng, and C. K. Tse, "Novel cubature Kalman filtering for systems involving nonlinear states and linear measurements," *International Journal of Electronics and Communications*, vol. 69, no. 1, pp. 314–320, 2014.
- [5] K. Reif, S. Gunther, and E. Yaz, "Stochastic stability of the discrete-time extended Kalman filter," *IEEE Transactions on Automatic Control*, vol. 44, no. 4, pp. 714–728, 1999.
- [6] S. Julier, J. K. Uhlmann, and H. F. Durrant-Whyte, "A new method for the nonlinear transformation of means and covariances in filters and estimators," *IEEE Transactions on Automatic Control*, vol. 45, no. 3, pp. 477–482, 2000.
- [7] K. Xiong, H. Y. Zhang, and C. W. Chen, "Performance evaluation of UKF-based nonlinear filtering," *Automatica*, vol. 42, no. 2, pp. 261–270, 2006.
- [8] K. P. B. Chandra, D.-W. Gu, and I. Postlethwaite, "Square root cubature information filter," *IEEE Sensors Journal*, vol. 13, no. 2, pp. 750–758, 2013.
- [9] J. Zarei and E. Shokri, "Convergence analysis of non-linear filtering based on cubature Kalman filter," *IET Science, Measurement & Technology*, vol. 9, no. 3, pp. 294–305, 2015.
- [10] I. Arasaratnam and S. Haykin, "Cubature Kalman filters," *IEEE Transactions on Automatic Control*, vol. 54, no. 6, pp. 1254–1269, 2009.
- [11] L. B. Chang, B. Q. Hu, A. Li, and F. J. Qin, "Transformed unscented Kalman filter," *IEEE Transactions on Automatic Control*, vol. 58, no. 1, pp. 252–257, 2013.
- [12] L. Zhang, H. B. Yang, H. P. Lu, S. F. Zhang, H. Cai, and S. Qian, "Cubature Kalman filtering for relative spacecraft attitude and position estimation," *Acta Astronautica*, vol. 105, no. 1, pp. 254–264, 2014.
- [13] D. Potnuru, K. P. B. Chandra, I. Arasaratnam, D.-W. Gu, K. A. Mary, and S. B. Ch, "Derivative-free square-root cubature Kalman filter for non-linear brushless DC motors," *IET Electric Power Applications*, vol. 10, no. 5, pp. 419–429, 2016.
- [14] S. Y. Wang, J. C. Feng, and C. K. Tse, "Spherical simplex-radial cubature Kalman filter," *IEEE Signal Processing Letters*, vol. 21, no. 1, pp. 43–46, 2014.
- [15] S. Bhaumik and Swati, "Cubature quadrature Kalman filter," *IET Signal Processing*, vol. 7, no. 7, pp. 533–541, 2013.
- [16] S. Bhaumik and Swati, "Square-root cubature-quadrature Kalman filter," *Asian Journal of Control*, vol. 16, no. 2, pp. 617–622, 2014.
- [17] B. Jia, M. Xin, and Y. Cheng, "High-degree cubature Kalman filter," *Automatica*, vol. 49, no. 2, pp. 510–518, 2013.
- [18] S. Das and J. M. Moura, "Distributed Kalman filtering with dynamic observations consensus," *IEEE Transactions on Signal Processing*, vol. 63, no. 17, pp. 4458–4473, 2015.
- [19] Z. W. Zhou, H. T. Fang, and Y. G. Hong, "Distributed estimation for moving target based on state-consensus strategy," *IEEE Transactions on Automatic Control*, vol. 58, no. 8, pp. 2097–2100, 2013.
- [20] R. Olfati-Saber, "Distributed Kalman filtering for sensor networks," in *Proceedings of the 46th IEEE Conference on Decision and Control*, pp. 5492–5498, New Orleans, La, USA, December 2007.
- [21] R. Olfati-Saber, "Kalman-consensus filter: optimality, stability, and performance," in *Proceedings of the 48th IEEE Conference on Decision and Control Held Jointly with the 28th Chinese Control Conference (CDC/CCC '09)*, pp. 7036–7041, IEEE, Shanghai, China, December 2009.
- [22] D. Alonso-Roman and B. Beferull-Lozano, "Adaptive consensus-based distributed Kalman filter for WSNs with random link failures," in *Proceedings of the International Conference on Distributed Computing in Sensor Systems*, pp. 187–192, New York, NY, USA, May 2016.
- [23] S. Das and J. M. F. Moura, "Consensus+innovations distributed Kalman filter with optimized gains," *IEEE Transactions on Signal Processing*, vol. 65, no. 2, pp. 467–481, 2017.
- [24] A. Pellett, *The extended Kalman-consensus filter [Ph.D. thesis]*, University of Maine, 2011.
- [25] I. Arasaratnam, S. Haykin, and R. J. Elliott, "Discrete-time nonlinear filtering algorithms using Gauss-Hermite quadrature," *Proceedings of the IEEE*, vol. 95, no. 5, pp. 953–977, 2007.

